

Lawrence Berkeley National Laboratory

Recent Work

Title

TURBULENCE IN THE POSITIVE COLUMN

Permalink

<https://escholarship.org/uc/item/1gm0b1n7>

Authors

Halseth, Martin W.

Pyle, Robert V.

Publication Date

1969-06-20

Submitted to Physics of Fluids

UCRL-19203
Preprint

cy. 2

RECEIVED
LAWRENCE
RADIATION LABORATORY
AUG 26 1969
LIBRARY AND
DOCUMENTS SECTION

TURBULENCE IN THE POSITIVE COLUMN

Martin W. Halseth and Robert V. Pyle

June 20, 1969

AEC Contract No. W-7405-eng-48

TWO-WEEK LOAN COPY

*This is a Library Circulating Copy
which may be borrowed for two weeks.
For a personal retention copy, call
Tech. Info. Division, Ext. 5545*

LAWRENCE RADIATION LABORATORY
UNIVERSITY of CALIFORNIA BERKELEY

UCRL-19203

cy. 2

DISCLAIMER

This document was prepared as an account of work sponsored by the United States Government. While this document is believed to contain correct information, neither the United States Government nor any agency thereof, nor the Regents of the University of California, nor any of their employees, makes any warranty, express or implied, or assumes any legal responsibility for the accuracy, completeness, or usefulness of any information, apparatus, product, or process disclosed, or represents that its use would not infringe privately owned rights. Reference herein to any specific commercial product, process, or service by its trade name, trademark, manufacturer, or otherwise, does not necessarily constitute or imply its endorsement, recommendation, or favoring by the United States Government or any agency thereof, or the Regents of the University of California. The views and opinions of authors expressed herein do not necessarily state or reflect those of the United States Government or any agency thereof or the Regents of the University of California.

TURBULENCE IN THE POSITIVE COLUMN*

Martin W. Halseth and Robert V. Pyle

Lawrence Radiation Laboratory
University of California
Berkeley, California

June 20, 1969

ABSTRACT

An oscillation that is helical in shape is known to be present when an axial magnetic field applied to the positive column of a glow discharge is greater than the critical magnetic field, B_c , for the onset of the current convective instability. According to a theory proposed by Kadomtsev, this oscillation will be replaced by a turbulent spectrum of oscillations when the field is several times B_c . In this experiment the magnetic field has been raised to as much as 20 times B_c to determine if and to what degree random oscillations characteristic of strong turbulence will replace the helical instability. It was found that strong turbulence dominated the positive column when the magnetic field was greater than 15 times the critical field. The radial mixing length as determined from spatial correlations with movable Langmuir probes and the radial density profile were found to agree with the results calculated from Kadomtsev's theory for strong turbulence. Partical transport rates calculated from the theories of Dupree and Kadomtsev for a turbulent plasma agree within a factor of two with the values deduced from this experiment.

I. INTRODUCTION

Particle losses in the positive column of a low-pressure glow discharge are known to be dependent upon the magnitude of the applied axial magnetic field. When the field is less than a critical value, B_c , the electric-field and charged-particle distributions were found to obey classical laws of transport.¹ At the critical field, Hoh and Lehnert discovered that the particle losses were greater than the classical theory had predicted.² Experiments by Allen, Paulikas, and Pyle³ in conjunction with the theory developed by Kadomtsev and Nedospasov⁴ proved that this anomalous rise in the electric field was the result of a current-convective instability associated with a helical density oscillation. Hoh has provided a detailed physical picture of the convective transport mechanism including the driving force provided by the axial separation of the ion and electron helices.⁵

Above the critical field, the behavior of the system becomes nonlinear. Holter and Johnson provided a theoretical description of the plasma when B is greater than B_c , assuming that the column would be dominated by a single fundamental helical density perturbation.⁶ Kadomtsev, whose definition of strong turbulence is used throughout this article, predicted that many interacting helical modes would be present, resulting in a strongly turbulent plasma when the magnetic field is many times the critical field.⁸ Although it is not possible for both of these theories to hold for the same experimental conditions, each can apply for a certain range of magnetic field strengths, with Kadomtsev's theory applying when B is very large compared to B_c .

Recently Dupree calculated the flux in the magnetized positive column when B is greater than B_c , using a model in which the phases of the particle orbits are incoherent.⁹ Dupree predicts that this model will describe radial transport whether there is one helical oscillation or several interacting modes in the plasma. This introduces another possible interpretation for data taken in the highly magnetized positive column.

Some measurements of spatial correlations of fluctuating density and voltage at values of the magnetic field as high as $20 B_c$ and of the radial density profile at three times B_c have been made by Wöhler.¹⁰ The results disagree with calculations made from the theory of Kadomtsev. Reasons for the disagreement are suggested in Section IVD.

Sheffield measured these same relevant parameters and others when the magnetic field was less than eight times B_c and determined that, with the possible exception of conditions at his highest applied field, the plasma was dominated by a single helical mode.¹¹ Robertson measured the local axial electric field in a cesium positive column, and at three times the critical field found some evidence, from the appearance of the plasma and the randomness of the field oscillations, that the column was turbulent.¹² Measurements by Nedospasov and Sobolev of the radial density profile at $8 B_c$ in a very low density plasma show a steep density profile in agreement with the theory of Kadomtsev.¹³

In our experiment we explore the nature of the instability in the positive column when the magnetic field is many times B_c . The radial and axial correlations, the frequency spectra, the density profile, and the electric field were measured. The data were taken at values of B/B_c which could not be reached in Sheffield's experiment, and the

results show a definite correlation with the predictions of Kadomtsev. The measurements, unlike those made by Wöhler, are sufficiently detailed that a distinction can be made between a plasma dominated by strong turbulence and one dominated by the presence of a single helix.

II. THEORY

The physical characteristics of the weakly ionized positive column are determined by the particle, energy, and momentum balances which occur in the system. For a plasma in which the Schottky theory¹⁴ applies, the diffusion will be classical when the magnetic field is less than B_c . The radial density profile is

$$n_0(r) = n(0)J_0(2.4r/a). \quad (1)$$

At the critical field, the time-dependent equations of particle and momentum conservation must be used. Kadomtsev and Nedospasov assumed a density distribution of the form

$$n(\underline{r}, t) = n_0(r) + n_1 J_1(3.83r/a) \exp[i(m\theta + kz - \omega t)] \quad (2)$$

and a potential distribution of similar form.⁴ Here $n_0(r)$ is the solution to the unperturbed equation. They substituted these distributions into the equations of momentum and continuity and linearized and combined the resulting equations to obtain such relevant quantities as the axial electric field.

When the magnetic field has been increased above the critical value, the interaction between the potential and density perturbations causes a change in the mean density profile in the plasma. For small

perturbations, the new "anomalous" diffusion can be calculated by using the previous forms for the density and potential fluctuations with a phase shift introduced between the two. Kadomtsev and Nedospasov performed such a quasilinear calculation in Ref. 4, assuming that the average density profile remains a zeroth-order Bessel function. By discarding this assumption, Holter and Johnson improved upon the calculation.⁶

Sheffield¹¹ created a model based upon that of Holter and Johnson which includes experimental values of the electric field and average radial density profile in the calculations. The fundamental helical mode is allowed a nonzero growth rate that is to be calculated from the theory. This implies that at some time the helix will break up, and a new helix will start to grow. He then obtained reasonable agreement with measured wavelengths, frequencies, and particle transport rates. The equation giving the particle transport is

$$q(r) = \frac{2J_1(\beta r)Zn(0)}{\beta^2 r(1+s)} \left[J_1(\beta r) + \frac{s\beta r}{2} \right] \times \frac{(1 + \mu_-^2 B^2)}{\mu_- B^2 (\mu_- + \mu_+)} \quad (3)$$

The radial profile of the oscillating portion of the density, $J_1(\beta r)$, defines the quantity β , which is of the order $1.5/a$. In Eq. (3) s is defined as

$$s = \frac{\frac{1}{4\pi n(0)E_z \mu_- a^2} - \left[\frac{J_1(\beta a)}{\beta a} \right]^2}{\frac{1}{2} \frac{J_1(\beta a)}{\beta a} - \frac{1}{4\pi n(0)E_z \mu_- a^2}} \quad (4)$$

and has a value from 0.5 to 2.0, depending upon the shape of the radial profile of the average density.

Kadomtsev has extended the theory of the unstable positive column to include the case of a positive column in a very high magnetic field.^{8,15} For this case he assumed that many oscillations of different wavelength and frequency may exist.

Plane geometry is used by Kadomtsev on the assumption, which must be proven by the results of the theory, that the derived radial correlation length will be small compared with the radius. Electron collisions can be ignored in the momentum equation for particles moving in the plane transverse to the column axis, and the extremely small ion-diffusion term may be eliminated. Perturbations of the same general form as in Eq. (2) are used. The resulting dispersion equation can be solved for the frequency of small amplitude oscillations:

$$\omega = \frac{k_z u(d_i/\alpha)}{d_e + d_i/\alpha} + i \frac{k_z \omega_* - d_e(d_i/\alpha)}{d_e + d_i/\alpha}, \quad (5)$$

where $u = -\mu_- E_z$, $\omega_* = (k_y T_- / m_- \Omega_-)(d \ln n / dx)$, $\alpha = T_+ / T_-$, $d_e = \tau_- k_z^2 T_- / m_-$, and $d_i = k_\perp^2 T_+ / (m_+ \Omega_+^2 \tau_+)$. The imaginary part of the frequency for $(\Omega_+ \tau_+)^2 \gg 1$ (which is true for the highest field used in this experiment) is

$$\gamma = \left[\left(\frac{\mu_- E_z}{\Omega_+ \tau_+} \right) \frac{d \ln n}{dx} \frac{k_y}{k_z} - D_- \frac{\mu_+}{\mu_-} \frac{k_\perp^2}{(\Omega_+ \tau_+)^2} \right] \frac{1}{1 + \frac{\mu_+}{\mu_-} \frac{k_\perp^2}{(\Omega_+ \tau_+ k_z)^2}}, \quad (6)$$

where $k_{\perp}^2 = k_x^2 + k_y^2$. The largest growth rate exists for that perturbation for which k_{\perp} is so small that the second term in Eq. (5) can be ignored and

$$\left(\frac{k_{\perp}}{\Omega_+ \tau + k_z} \right)^2 \frac{\mu_+}{\mu_-} \equiv X' = 1 \quad (7)$$

and $k_y \approx k_{\perp}$. Then we have

$$\gamma = U \frac{d \ln n}{dx} \quad (8)$$

where

$$U = \frac{1}{2} E_z (\mu_- \mu_+)^{1/2}. \quad (9)$$

An analogy with hydrodynamics (Prandtl¹⁶) was drawn at this point by Kadomtsev to associate these perturbations with measurable quantities in a chaotic plasma. Because of the spectral continuum of wavelengths in the plasma, coherent oscillations are impossible outside a small region or cell in the plasma. This cell can be characterized by an effective mixing length l , as in ordinary turbulence. Similarly, the density fluctuation can be written as $n' = l dn/dr$, and its speed will be $v' = Un'/n$. Kadomtsev assumed that, for insulating walls that have no stabilizing effect on the fluctuations, l may be taken as constant for a given tube.

The flux of particles in a cylindrical system can be written (ignoring collisional transport)

$$q = n'v' = D dn/dr, \quad (10)$$

where $D = v'l = \gamma\ell^2$. Here the value of γ calculated in the Cartesian system can be used on the basis of the previous hypothesis. The equation of continuity,

$$\frac{1}{r} \frac{d}{dr} (rq) = nZ, \quad (11)$$

can be solved for n with the boundary conditions $n(0) = n_0$, $n'(0) = 0$, and $n(a) = 0$. The result is a density profile $n(r) = n(0)y_0(x_0r/a)$, where the root is

$$\left(\frac{Za^3}{\ell^2 U} \right)^{1/3} \equiv x_0 = 3.40, \quad (12)$$

and the flux is

$$q(r) = \frac{U\ell^2}{n(r)} \left(\frac{dn}{dr} \right)^2. \quad (13)$$

Kadomtsev has calculated a value of Z to use in Eq. (12) by first considering a second column of radius a_1 at the same pressure and electric field but without an applied magnetic field. In this tube, the ionization rate and electron temperature are the same as in the tube of radius a if one ignores turbulent heating, which, as will be seen below, is a reasonable assumption in this problem. In the stable column we have

$$Z = \frac{\mu_+}{\mu_-} \frac{T_{\mu_-} (2.4)^2}{ea^2}. \quad (14)$$

Then using Eq. (12), we can write

$$\ell^2 = \frac{2a^3 T_- (2.4)^2}{x_0^3 e a_1^2 E_z} \left(\frac{\mu_+}{\mu_-} \right)^{1/2} \quad (15)$$

Using the results of previous experiments which measured E_z for $B \gg B_c$, Kadomtsev calculated typical values of ℓ/a which were of the order of 0.15. Kadomtsev has shown also that the fluctuations of the total electric field, which measure the heating of the electrons by the oscillations, are of the order of $(\ell/a)E_z$, so that turbulent heating has very little effect on the electron temperature and can be ignored.

Another boundary condition, suggested by an experiment by Artsimovich and Nedospasov,¹³ was used by Kadomtsev in Ref. 8. Since, in all experiments, the density in the turbulent column is found to be nonzero near the wall, Kadomtsev proposes that an extrapolated boundary-length condition be imposed. Then q/U equals the density at the wall, and the extrapolated boundary length is $\ell' = \left\{ \left[\frac{d(\ln n)}{dr} \right]_{r=a} \right\}^{-1}$. This leads to the relation $\ell' = \ell$ and a new value for a to be used in Eq. (15) which is the distance between the center of the tube and the point outside the tube where the extrapolated density goes to zero. This distance may be approximated by the sum of the tube radius and the mixing length.

Sato¹⁷ extended Kadomtsev's analysis and derived an axial correlation length $\ell_{||}$. Sato assumes that the condition $X' = 1$ is merely a description of the onset of turbulence, and that $\ell_{||}$ and ℓ are independent of B , but γ and E are not. Then, assuming $k_{\perp}/k_z = \ell_{||}/\ell$, Sato found that

$$l_{||} = l(\mu_{-}\mu_{+})^{1/2} B_{X'=1} \quad (16)$$

With the restriction on X' removed, γ becomes, for very large magnetic fields, proportional to B^{-1} , as does the diffusion coefficient. In this case the electric field should decrease as the magnetic field increases.

Hoh suggests that the single helix of the quasilinear region will break up into many high-frequency helical modes, and concludes that all of these will possess the same growth rate.¹⁸ The many modes will result in a plasma that is in a strongly turbulent state similar to that predicted by Kadomtsev.

Dupree has used an entirely different model of the positive column.⁹ He, too, arrives at the same basic linear equation (5) for a particular mode of oscillation as does Kadomtsev. The collisional damping decrements $d_{e,i}$, unlike those derived in the linear theory of Kadomtsev, include wave contributions $d_{\omega e, \omega i}$ in Dupree's theory. The nonlinear features of the plasma have been accounted for in these additions to the damping decrements. The decrements may be calculated in terms of $\text{Re}(\omega)$ if the growth rate is set equal to zero.

The radial flux is essentially the convective flux, which Dupree calculates:

$$q(r) = \frac{-d_{\omega, e}}{2k_r^2} \left(1 - \frac{\omega - k_z u}{\omega^*} \right) \frac{\partial n}{\partial r} \quad (17)$$

Here k_r is the radial wave number, which Dupree takes as $1.2\pi/a$, since the radial standing wave is essentially an approximation to $J_1(3.83r/a)$.

From the experimental data, the total radial flux can be calculated and compared with the experimental value. The theory does not predict such quantities as frequency, wavelength, and electric field, but requires experimental values for these terms.

Equation (15) and the density profile from Kadomtsev's theory of turbulence, $y_0(x_0 r/a)$, provide numerical results which can be easily compared with experiment. The best experimental test for the absence of the helical $m = 1$ mode is a check of Eq. (2) by the use of correlation techniques. If no dominant oscillation is present, and instead the spectrum is a broad continuum of frequencies, the system is turbulent. Then one can check to find out if results compare with the predictions by Kadomtsev about strong turbulence. Calculations of the loss rate [Eqs. (3), (13), and (17)] will be compared with the measured production rate in the plasma.

III. EXPERIMENTAL EQUIPMENT AND PROCEDURE

A. Apparatus

The basic arrangement used throughout this experiment is shown in Fig. 1. The Pyrex discharge tube used had a length of 300 cm and a radius of 2.75 cm. Two easily removed electrodes were attached to the end of the tube by means of ground-glass joints sealed with Apiezon wax. At low pressures, the length of the tube was increased 2 m to reduce the effects of the ends on the conditions in the central axial region of the plasma, where most experiments were performed.

The magnetic field was provided by ten 9-in.-i.d. water-cooled coils 6 in. wide and spaced 2.25 in. apart. Photomultiplier monitoring and probe insertion took place between the coils. With one power

supply of the type available, the maximum axial field was 7 kG. Fields up to 12 kG were obtained by splitting the coils into three groups of three and using three power supplies.

The vacuum was provided by a 4-in. oil-diffusion pump in conjunction with a refrigerated baffle system and liquid-nitrogen cold trap. The base pressure of this system was 10^{-7} mm Hg. Control of the helium pressure inside the tube was maintained by regulation of the exit valve near the grounded electrode and of the bleed valve through which the gas was continuously fed. Any significant impurities in the system were flushed out by running the discharge for an hour before data were recorded. Satisfactory purity was signified by a deep pink glow throughout the column. The neutral gas pressure was measured with an Autovac gauge.

At various times several movable double Langmuir probes were inserted in the plasma. Their locations are shown in Fig. 1. The axial probe was a dogleg probe which rested on the bottom of the column, except for the 8-cm-long double bend, and reached from the anode to slightly past the center of the tube. Except when axial correlations were being measured, the radial probes were bent parallel to the axis of the discharge tube several centimeters before the probe tips. Continuous frequency spectra were taken on a Nelson-Ross spectrum analyzer unit built for a 551 Tektronix oscilloscope. Both the azimuthal electric field and the ion saturation current were analyzed.

The two probe wires were covered by separated slender glass sleeves for 3 cm, terminating at the tips in 2-mm-long bare wires

separated by 1 mm (Fig. 1). The wires of 0.125-mm diameter molybdenum were protected by a larger single glass sleeve after the separate sleeves. This joined to a 6-mm glass tube which could be moved by means of a calibrated gear mechanism in the case of the radial probe. The system used to measure the current between the two ends of a double probe is described in Ref. 19.

Radial spatial correlation measurements were made with two probes entering radially from opposite sides of the tube. Signals from the two probes were amplified to the same rms value and then put into a special function summer,¹⁹ which provided the rms values of the sum and difference of the two signals. The difference of the squares of these two values divided by the sum of the squares provides the normalized correlation of the two signals. The equation for finding the correlation is

$$\begin{aligned}
 R_{AB} &\equiv 2\langle(\tilde{\delta}_A \tilde{\delta}_B)\rangle / (\langle\tilde{\delta}_A^2\rangle + \langle\tilde{\delta}_B^2\rangle) \\
 &= \frac{\langle(\tilde{\delta}_A + \tilde{\delta}_B)^2\rangle - \langle(\tilde{\delta}_A - \tilde{\delta}_B)^2\rangle}{\langle(\tilde{\delta}_A + \tilde{\delta}_B)^2\rangle + \langle(\tilde{\delta}_A - \tilde{\delta}_B)^2\rangle}, \quad (18)
 \end{aligned}$$

where $\tilde{\delta}$ is the fluctuating part of the quantity δ .

Photomultiplier tubes were used to measure the time-dependent light intensity. They provided a check of the signals from the Langmuir probes. A radial bank of tubes was also used to detect azimuthal phase shifts necessarily present if the oscillations are helical.

IV. RESULTS AND DISCUSSION

A. Longitudinal Electric Field

The axial electric field in the positive column was measured in two independent ways. The potential difference between the two electrodes and the potential difference measured by a movable probe between two axial positions on the same field line were both used as sources of axial electric field values. Results of the measurements for pressures of 80, 200, and 400 mTorr are shown in Fig. 2.

According to the theory of Kadomtsev, the electric field should no longer be affected by the magnetic field when the plasma is strongly turbulent. Within experimental accuracy the results show agreement with this theory when the ratio of B to B_c is large. There is no indication of a $1/B$ dependence when the field is very high.

Neither measuring technique is without error. The total potential drop across the length of the tube gives an upper limit to the electric field because the electric field is higher outside the magnetic field.

The axially movable probe was observed to affect the plasma potential and the critical magnetic field slightly, and there was difficulty in keeping the probe on the same field line during the measurements, resulting in errors in the calculated electric field. Since the possible error resulting from a gross error in the placement of the probe was less than 1 V, the error caused by misalignment, if the electric field was measured over a distance of 30 m, must have been about 3%.

There is, therefore, some uncertainty in the slope of $E_z(B)$,

particularly at high magnetic fields where E_z changes slowly with B . Since the axial probe data were taken near the center of the tube, these were the measurements used in calculations of the turbulent decay length in Section IV D.

B. Radial Density Profiles

Measurements of the relative ion density as a function of radius have been made in the positive column in the pressure range from $p = 20$ to $p = 400$ mTorr. Results for several pressures are shown in Figs. 3 and 4 for magnetic fields up to $B = 12$ kG in a constant discharge current of 400 mA. In fig. 4 results are included for a different current, $I = 200$ mA, when B is 12 kG, and the results are similar to those for $I = 400$ mA. For the sake of comparison, the J_0 Bessel function and function $y_0(x_0 r/a)$ of Kadomtsev's turbulence theory are included.

The measured profiles were symmetric about the center of the plasma, which was found to be always within 2 or 3 mm of the geometric center of the tube. Because of the size of the probe stem, density measurements were excluded from the region within about 0.5 cm from the wall.

The data at the highest values of B/B_c considered agree with the Kadomtsev profile $y_0(x_0 r/a)$. The flattening of the profile at lower field ratios, e.g., when $B = 12$ kG and $p = 400$ mTorr or when $B = 7$ kG and $p = 200$ mTorr, is in agreement with theories that assume the presence of a dominant helical instability at such fields.

The conditions in Fig. 3 are quite similar to those in an experiment by Nedospasov and Artsimovich¹³ in which, from the close

correspondence of their radial profile to that of the theory, they deduced that agreement was obtained with the turbulence theory of Kadomtsev.⁷ The criterion of Simon²⁰ for ambipolar diffusion is violated, however, by the relatively small ratio of length to radius for their pressure (20 mTorr) and magnetic field.

A longer tube, with 2 meters of the cathode end extending outside the field, was used during part of the present experiment. Although this added length does not guarantee satisfaction of the Simon criterion, it does eliminate cathode effects and reduce the number of fast electrons in the field region. Density profiles shown in Fig. 3 imply that these effects are absent in the shorter tube.

C. Oscillation Spectra

The spectrum of azimuthal-electric-field oscillations and spectrum of density oscillations were recorded with the spectrum analyzer when the radial double probe was located 1.5 cm from the center. This position was always near the maximum in the helical fluctuation intensity. Typical results are shown in Fig. 5. The results in the field range dominated by the helix agree with results reported by Sheffield and by Nedospasov and Sobolev.²¹ No fluctuations, including striations, were found when the field was lower than the critical field, provided the pressure was not greater than 400 mTorr. No indication of prominent harmonics of the fundamental helical mode were found.

An $m = 0$, i.e., azimuthally symmetric, mode is observed in the positive column when the magnetic field is greater than the critical value. This oscillation (not a striation), which Huchital and Holt²²

discovered experimentally, is associated with any small transverse magnetic field that may be present, perhaps because of a slight misalignment between the electric and magnetic fields. It is measured along with the helical oscillation when density fluctuations are observed. To eliminate contributions from the $m = 0$ mode, only azimuthal electric-field fluctuations were recorded. Because of imperfect common-mode rejection by the measuring system, not all of the $m = 0$ mode could be excluded.

At 12 kG, for all pressures except 400 mTorr, the spectra give no indication that they are dominated by any single oscillation. The spectra are continuous, implying the presence of turbulent fluctuations. At lower fields, the spectra are dominated by a single oscillation at the frequency of the first helical mode. For example, see Fig. 5. For a field of 2.1 kG, at a pressure of 120 mTorr, this frequency is 18 kHz. The frequency spectrum is particularly sharp when B is near B_c .

Kadomtsev's theory of strong turbulence also predicts the approximate value for the maximum in the turbulence spectrum. The frequency for which the growth rate is the greatest is

$$f = \frac{-\mu_-}{(1 + X'^2)} \frac{1}{\lambda_{\parallel}} \left[E_z + \frac{T_- X'}{(\mu_-/\mu_+)^{1/2}} \frac{d \ln n}{dx} \right]. \quad (19)$$

The value of X' can again be taken as 1. The axial wavelength can be found from Eq. (7). The value of k_{\perp} is the minimum possible, so λ_{\parallel} must be a maximum and may be approximated by the length of the tube.

The calculated value for the conditions which apply to the 12 kG curve in Fig. 5 is 16 kHz, which is about twice the measured frequency corresponding to the maximum amplitude of the spectrum.

D. Correlations

Both radial and azimuthal correlations were obtained at magnetic fields up to 12 kG in the positive column. Radial density correlations (R_{\perp}) were taken for pressures ranging from 80 to 400 mTorr and a current of 400 mA; typical results are shown in Figs. 6 and 7. The points were taken with the fixed probe located 1 cm into the plasma. This permitted data to be taken with the movable probe on the opposite side of the axis.

Small negative correlations are observed at 12 kG when the probes are 180 deg apart. These may be attributable to experimental error, since the possible error in the correlating electrons is about 10%. The fact that all results are similar, however, would indicate that a small portion of the fundamental helix does remain.

At magnetic fields lower than 12 kG, the helical mode is clearly stronger than at 12 kG. The signals would be 180 deg out of phase on the two probes when the probes are on opposite sides of the axis, except for the presence of the $m = 0$ mode. The shape of the radial correlation at 7 kG suggests that there is some strong turbulence in the plasma.

In order to determine the relative amounts of $m = 0$ and $m = 1$ fluctuation, density correlation measurements were made between a radial probe and an axial probe separated by 90 deg and both located

at the same axial position and 1.5 cm from the center. Unless the system is turbulent, the positive value of the correlation is the fraction of the oscillations in the plasma that are azimuthally symmetric. In the case of turbulence, the correlation is a measure of the transverse decay in the spatial correlation. Results are given in Table I. The low values of the 90-deg correlation at high fields indicate that the azimuthally symmetric mode is essentially absent.

To determine the degree of homogeneity of the plasma turbulence, the results obtained when the fixed probe was 1 cm from the wall nearest its entrance port were compared with measurements of the radial correlation with the fixed probe located 3 mm from the center on the same side as the movable probe. A comparison of the results at 12 kG¹⁹ indicates that the turbulence is homogeneous in a region within 2 cm of the tube center.

Wöhler¹⁰ has made correlation measurements in helium for a pressure of 150 mTorr when $B/B_c = 20$ and found $l \approx a$. These measurements were made on only one side of the axis. As a result, if a helical mode were dominant, rather than strong turbulence, this fact could not be determined from the data. Fluctuations were measured with straight probes. There is a real possibility that, because the support arms were on the same radial line as the probe, there was strong interference between the probes.

A comparison between straight and bent probes has been made in the present experiment. The difference in results obtained when straight double probes are used in correlation measurements instead of

the bent probes, which isolate the data-gathering probe tips from the bulky entrance segments of the probes, is shown in Fig. 8. The increase in correlation is quite probably a result of the interference between the two entrance lengths, which are at the same axial positions as the probe tips.

To determine the effect of the finite size of the probe tip on the measurements, radial correlations were made with 0.050-mm-diam probe tips under the same conditions as those for the 0.125 mm tips (Fig. 7). Results are similar for the two probe radii, suggesting that the size of the probes used has little effect on the measurements.

To a good approximation a spatial-correlation curve in fluid turbulence is an exponentially decreasing function of separation, and so the mixing length may be taken as the exponential decay length of the correlation function. By analogy, the mixing length in this experiment may be obtained by fitting the data to a decaying exponential and ignoring the region of negative correlations. Figure 9 shows the calculated length at 12 kG. Also included is the mixing-length curve predicted in Kadomtsev's theory for the turbulent positive column and obtained with the aid of the measured electric field at 12 kG.

The electron temperature used in our calculations was found from experimental values of T_e as a function of E_z/p as deduced from Refs. 1 and 11. The ionization rate, Z , was calculated from the von Engel and Steenbeck relation, which for atomic helium is

$$Z = 6.15 \times 10^6 p T_e^{-3/2} \left(\frac{24.5}{2T_e} + 1 \right) \exp \left(- \frac{24.5}{T_e} \right) \quad (20)$$

ionizations per electron per second.¹ In his equation for the correlation length (12) Kadomtsev has used the Schottky condition for Z (14), and the resulting values of Z may be twice as large as those calculated from Eq. (20) at low pressures. It has been assumed in all calculations but those for ℓ that Eq. (20) will apply even in the presence of a strong magnetic field. Curves using both calculations of Z are shown in Fig. 9.

If the $m = 1$ mode is still strong at high pressures, at which B/B_c is less for a given B , the radial correlation is dominated by the helical oscillation rather than the random oscillations also present. The mixing length taken from the data is then greater than it would be for strong turbulence, because the effect of the helix is to yield values of the correlation that are close to one when the two probes are on the same side of the axis. Then the apparent mixing length should increase with pressure for high pressures, as shown in Fig. 9, in opposition to the predicted trend in the case of strong turbulence.

The fit with the calculations made from the turbulence theory of Kadomtsev of the measured radial density profiles and radial correlation lengths provides definite evidence of the presence of oscillations characteristic of strong turbulence when B is 12 kG. The correlation measurements made here at 12 kG disagree with the results of Wöhler¹⁰ as mentioned previously (Fig. 8).

Axial correlation measurements were obtained in the same manner as were the radial data. Results are shown in Fig. 10. The fixed radial probe was straight, with only the tips bent along the field lines.

Results of axial density correlations could be ambiguous because there are two types of oscillations present, one of which, the $m = 0$, is azimuthally symmetric. However, if data are taken with the mobile axial probe separated azimuthally by 180 deg from the fixed probe's field line as well as being taken with the probe near the field line, the two modes can be separated. The correlation between one signal and a second signal at another axial position is independent of the azimuthal separation in the case of the $m = 0$ wave, and proportional to the cosine of the azimuthal separation for the $m = 1$ wave. The wavelength and the amount of axial decay of the helix can be found from the weighted difference between the two correlations, assuming that no higher modes exist and that the $m = 0$ mode is perfectly correlated radially:

$$R_{\parallel, m=1}(z_1, z_2, \theta = 0 \text{ deg}) = \frac{R_{\parallel}(z_1, z_2, \theta = 0 \text{ deg}) - R_{\parallel}(z_1, z_2, \theta = 180 \text{ deg})}{R_{\parallel}(z_1, z_1, \theta = 0 \text{ deg}) - R_{\parallel}(z_1, z_1, \theta = 180 \text{ deg})} \quad (21)$$

Results are shown in Table II.

Included in Table II are calculations of the axial wavelength found by using the linear theory of Johnson and Jerde²³ when $B = B_c$ and the quasilinear semi-empirical theory of Sheffield when the $m = 1$ mode was dominant and $B > B_c$. Wavelengths which were measured at the critical field agree with the theory (Table II), and the signal shape (Fig. 10) is a reasonable approximation to a cosine, although a large $m = 0$ mode was present in the plasma, indicating that separation of the two modes was obtained.

When the magnetic field is at 12 kG, both the correlation along the field line (Fig. 41 of Ref. 19) and the correlation used in Fig. 10, except in the 400 mTorr case, indicate absence of both the helix and the azimuthally symmetric oscillation. Decay lengths measured by fitting exponential curves to the axial correlation data at 12 kG were included in Table II (an average value of the results such as those from Fig. 10 and Fig. 41 of Ref. 19 was used), and the results were compared with the calculation of $l_{||}$ made with Eq. (16).

The segments of the positive column at the ends of the magnetic-field region were affected by the diverging or converging field lines. End effects resulted in changes in the plasma color at the anode end and separation of the plasma from the wall at the cathode end. The work of Nedospasov and Sobolev²¹ in the quasilinear region suggests that it would be worthwhile to suppress these entrance phenomena at the cathode end and study the resulting effects upon oscillations at all values of the magnetic field. Axial measurements in this experiment were confined to the large central section of the plasma where entrance effects were absent.

No measurements were made in the dc plasma at pressures above 400 mTorr because of the presence of striations and the low value of B_{\max}/B_c .

E. Particle Transport

Radial transport may be calculated from many of the theories of the unstable positive column. Among these, the theory of Sheffield provides an estimate of the radial flux at any radius whenever the

plasma is dominated by the $m = 1$ helix. The semi-empirical theory of Sheffield is used in these calculations in preference to other quasilinear theories, such as that of Holter and Johnson, because of the treatment of the radial density profile by Sheffield. Fitting the profile to the measured value as Sheffield has done allows the wall density to be nonzero, as it is in this experiment.

If the radial density profile is steeper than $J_0(2.45r/a)$, then quasilinear theories of the positive column^{4,6,11} are inapplicable, since they assume the presence of the zeroth-order Bessel distribution plus some contribution from the helical mode which broadens the profile. When the plasma is strongly turbulent, transport can be calculated from either Kadomtsev's or Dupree's theory. When the oscillations in the plasma are clearly not random, however, Kadomtsev's theory is invalid.

The two regions of instability are both covered by the work of Dupree. A mean wavelength and frequency for use with the model of Dupree can be measured even when $B = 15B_c$, although the amplitude level is very small compared to the total level of oscillations.

The experimental values of the particle flux used in the comparison with theoretical fluxes are deduced from the values of the production rate, which is a function of the experimental values of E_z and $n(r)$. The production rate, q_p , is

$$q_p(\rho) = Z/\rho \int_0^\rho n(r)rdr, \quad (22)$$

which must equal the particle flux through a unit area on a cylinder

located at $r = \rho$.

The formulas to be used are Eqs. (3), (13), and (17), and the radius at which the flux is calculated is $0.6a$, where the instability appears to be strongest. Results are given in Table III.

At high values of B/B_c the density profile used in the Sheffield model is in contradiction to experiment. Otherwise, this quasilinear theory fits the data. The calculations from the theory of Dupree approximate the experimental loss rates within a factor of 2 for all the measurements made here. Kadomtsev's theory shows agreement only at 12 kG. For $B/B_c < 10$ the measured radial correlation lengths are so large that Kadomtsev's theory should not be applied.

V. SUMMARY AND CONCLUSIONS

Application of a magnetic field with a value greater than 15 times the critical field to a positive column is shown to produce a turbulent plasma with parameters that compare closely with the predictions from Kadomtsev's theory of turbulence in the positive column. Transport is dominated by the radial convection of charged particles under the influence of random oscillations of the electric field in accordance with this theory. For fields with lower values, convection caused by the helical instability rather than turbulent convection appears to be the dominant transport mechanism, in agreement with other experiments.^{3,11} When B is raised above $10 B_c$, the fluctuations in the plasma change continuously from helical oscillations to turbulent oscillations.

Particle transport when the magnetic field is greater than $3 B_c$ is a very slowly varying function of B , as can be seen in Table III.

The various theoretical predictions of radial flux appear to be reliable within a factor of two within their ranges of applicability. Kadomtsev's and Dupree's theories of turbulence both provide reasonable estimates of particle transport in the positive column for $B \gg B_c$.

The close fit between experimental and theoretical values of the mixing length and the density profile at very high magnetic fields shows that the Kadomtsev model of turbulence in the positive column fits the conditions of this experiment. In this case, transport is a matter of small turbulent cells convecting radially outward with an average velocity determined by their size and growth rate. A better description of transport, however, should include the effects of inhomogeneous turbulence at the boundary. Such an analysis would avoid the need to invent an extrapolation-length boundary condition such as that used by Kadomtsev. Nevertheless, the results do indicate that a model of turbulence analogous to the hydrodynamic model can be used to describe the positive column for $B/B_c > 15$.

ACKNOWLEDGMENTS

We wish to thank Prof. Wulf B. Kunkel, Dr. Roy R. Johnson, Prof. Thomas H. Dupree, and Dr. Laird Warren for valuable discussions of the theory and experiment. We are also grateful to Vincent J. Honey and Donald B. Hopkins for the design and construction of much of the electronic equipment used in this experiment and to Dr. C. M. Van Atta for his support of this research. The skill and dedication of the personnel in Harry Powell's glass shop, especially Ione Maxwell, and the mechanical shops of Louis A. Biagi and Harlan Hughes were essential to the success of this work.

FOOTNOTES AND REFERENCES

*This work was done under the auspices of the U. S. Atomic Energy Commission.

1. R. J. Bickerton and A. von Engel, Proc. Phys. Soc. (London) 68, 468 (1955).
2. F. C. Hoh and B. Lehnert, in Proceedings of the 4th International Conference on Ionization Phenomena in Gases, Uppsala (North-Holland Publishing Co., Amsterdam, 1960), p. 604.
3. T. K. Allen, G. A. Paulikas, and R. V. Pyle, Phys. Rev. Letters 5, 409 (1960).
4. B. B. Kadomtsev and A. V. Nedospasov, J. Nucl. Energy, Pt. C, 1, 230 (1960).
5. F. C. Hoh, Phys. Fluids 5, 22 (1962).
6. Ø. Holter and R. Johnson, Phys. Fluids 8, 333 (1965).
7. B. B. Kadomtsev, Plasma Turbulence (Academic Press, New York, 1965).
8. B. B. Kadomtsev, Soviet Phys.-Tech. Phys. 6, 927 (1962).
9. T. H. Dupree, Phys. Fluids 11, 2680 (1968).
10. K. Wöhler, Phys. Fluids 10, 245 (1967).
11. J. Sheffield, Phys. Fluids 11, 222 (1968).
12. H. S. Robertson, Diffusion of Plasma Across a Magnetic Field, AFCRL-64-277, 1964.
13. L. A. Artsimovich and A. V. Nedospasov, Doklady Akad. Nauk. S.S.S.R. 7, 717 (1963).
14. W. Schottky, Physik. Z. 25, 635 (1924).
15. B. B. Kadomtsev, Soviet Phys.-Tech. Phys. 6, 882 (1962).

16. L. Prandtl, The Essentials of Fluid Dynamics (Blackie, London, 1952).
17. M. Sato, AERE Transl. 924 of Kaku-Yuge Kenkyu 8, 563 (1962).
18. F. C. Hoh, in Plasma Instabilities and Anomalous Transport, W. B. Pardo and H. S. Robertson, eds. (University of Miami Press, Coral Gables, Fla., 1966), pp. 207-17.
19. M. W. Halseth, Turbulence in the Positive Column of a Glow Discharge (Ph.D. thesis), Lawrence Radiation Laboratory Report UCRL-18678, February 1969.
20. A. Simon, Phys. Rev. 98, 317 (1955).
21. A. V. Nedospasov and S. S. Sobolov, Soviet Phys.-Tech. Phys. 11, 1309 (1967).
22. D. A. Huchital and E. H. Holt, Phys. Rev. Letters 16, 677 (1966).
23. R. R. Johnson and D. A. Jerde, Phys. Fluids 5, 988 (1962).

Table I. Fraction of signal that is azimuthally symmetric.

B (kG)	P (mTorr) = 80	120	200	300	400
1.4	0.16	0.21	0.38	0.59	0.48
3.5	0.07	0.25	0.32	0.03	0.14
7.0	0.05	0.11	0.09	0.03	0.21
12	0.04	0.07	0.05	0.07	0.04

Table II. Axial wavelength and correlation length.

p (mTorr)	B (kG)	λ (cm)		l (cm)	
		Measured	Computed	Measured	Computed
80	$B_c = 0.560$	140	170	--	--
	3.5	260	150	--	--
	12	---	---	23	71
120	$B_c = 0.630$	100	130	--	--
	5.6	180	220	--	--
	12	---	---	12	42
200	$B_c = 0.710$	80	100	--	--
	5.6	180	130	--	--
	12	---	---	30	21
300	$B_c = 0.805$	80	80	--	--
	7	170	110	--	--
	12	---	---	28	13
400	$B_c = 0.910$	70	70	--	--
	7	200	80	--	--
	12	200	80	--	11

Table III. Radial particle transport rates. Blanks indicate that the assumptions used are incompatible with experimental conditions.

p (mTorr)	B (kG)	Transport rates (10^{14} particles/cm ² -sec)			
		Sheffield	Dupree	Kadomtsev	Experiment
120 ($B_c = 630$ G)	3.5	22	14	---	21
	7	25	33	310	23
	12	--	49	48	31

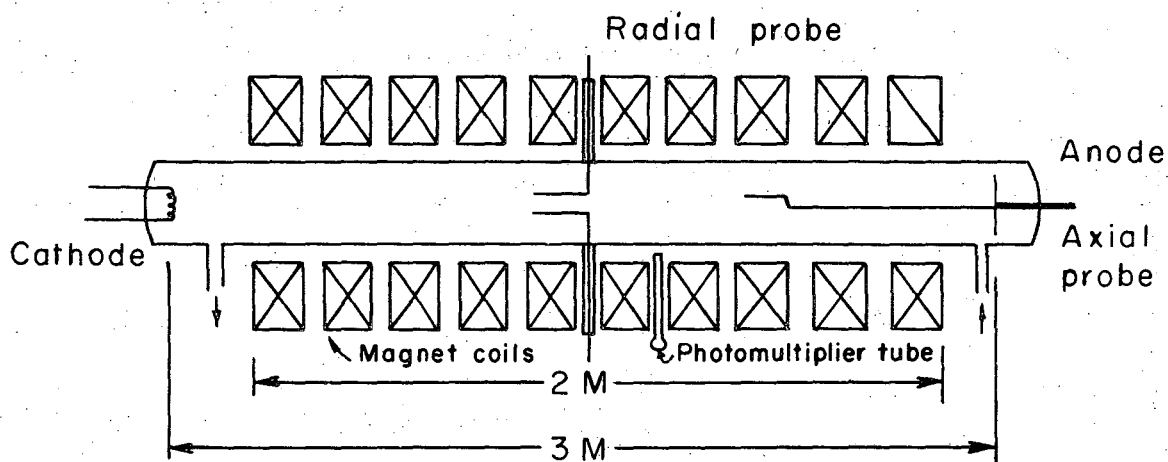
200 ($B_c = 710$ G)	3.5	18	10	---	20
	7	20	20	210	20
	12	--	29	36	26

300 ($B_c = 805$ G)	3.5	13	9	---	14
	7	14	15	---	17
	12	20	14	20	18

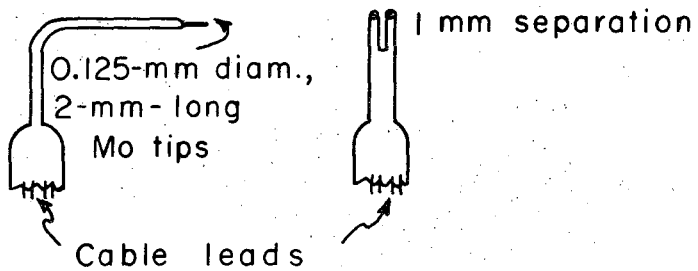
- Fig. 1. Schematic of positive column experiment and probe construction.
- Fig. 2. Electric field as measured by a probe (Δ) and as measured from the interelectrode potential (\square). (a), $p = 80$ mTorr; (b), $p = 200$ mTorr; (c), $p = 400$ mTorr. The curves are drawn to aid the reader.
- Fig. 3. Normalized density profile. $p = 20$ mTorr, $B_c = 250$ G.
 \bullet , $b = 2.1$ kG, tube 5 m long; \square , $B = 1$ kG, tube 5 m long;
 \circ , $B = 1$ kG, tube 3 m long; Δ , $B = 0$, tube 3 m long.
- Fig. 4. Normalized density profile. $p = 200$ mTorr, Δ , $B = 0$ kG;
 \square , $B = 3.5$ kG; \blacktriangle , $B = 7$ kG, \circ , $B = 12$ kG; all at $I = 400$ mA.
 \bullet , $B = 12$ kG, $I = 200$ mA.
- Fig. 5. Fluctuating azimuthal-electric-field spectra. $p = 120$ mTorr.
- Fig. 6. Radial density correlation vs radial separation. $p = 80$ mTorr. \bullet , $B = 2.1$ kG; Δ , $B = 3.5$ kG; \square , $B = 7$ kG; \circ , $B = 12$ kG. Curves are drawn through points for $B = 2.1$ and 12 kG to aid the reader.
- Fig. 7. Radial density correlation vs radial separation. $p = 200$ mTorr. \bullet , $B = 2.1$ kG; \square , $B = 7$ kG; \blacktriangle , $B = 10$ kG; \circ , $B = 12$ kG; all data measured using 0.125-mm diameter probe tips.
 Δ , $B = 12$ kG; probe tip diameter = 0.050 mm. Curves drawn through the points for $B = 2.1$ and 12 kG to aid the reader.
- Fig. 8. Radial density correlation vs radial separation. $p = 200$ mTorr; $B = 12$ kG. \bullet , bent probe (standard configuration used in experiment); Δ , straight probe, with curves drawn to aid the reader.

Fig. 9. A comparison between the radial mixing length as a function of pressure as calculated from Kadomtsev's theory of turbulence (solid curves) and the radial correlation length as measured in this experiment (o). For curve (a) Z was calculated using Eq. (14), and for curve (b) Z was calculated using Eq. (20).

Fig. 10. Adjusted axial-density correlation vs axial separation. $p = 200$ mTorr. All curves drawn to aid the reader. The curve for $B = B_c$ is fit to a cosine shape. \square , $B = B_c$ (700 G); Δ , $B = 5.6$ kG; o , $B = 12$ kG.

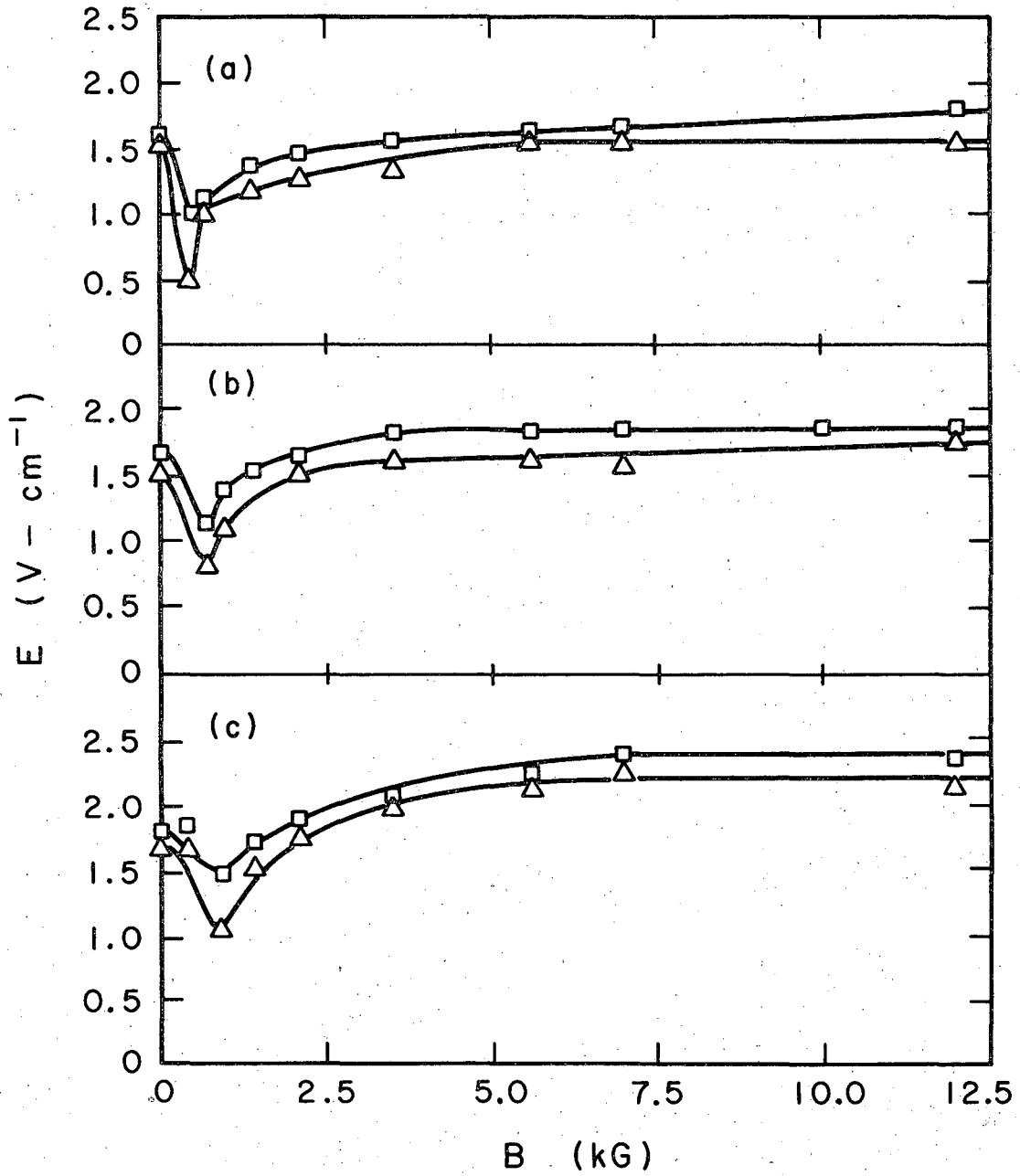


Probe construction



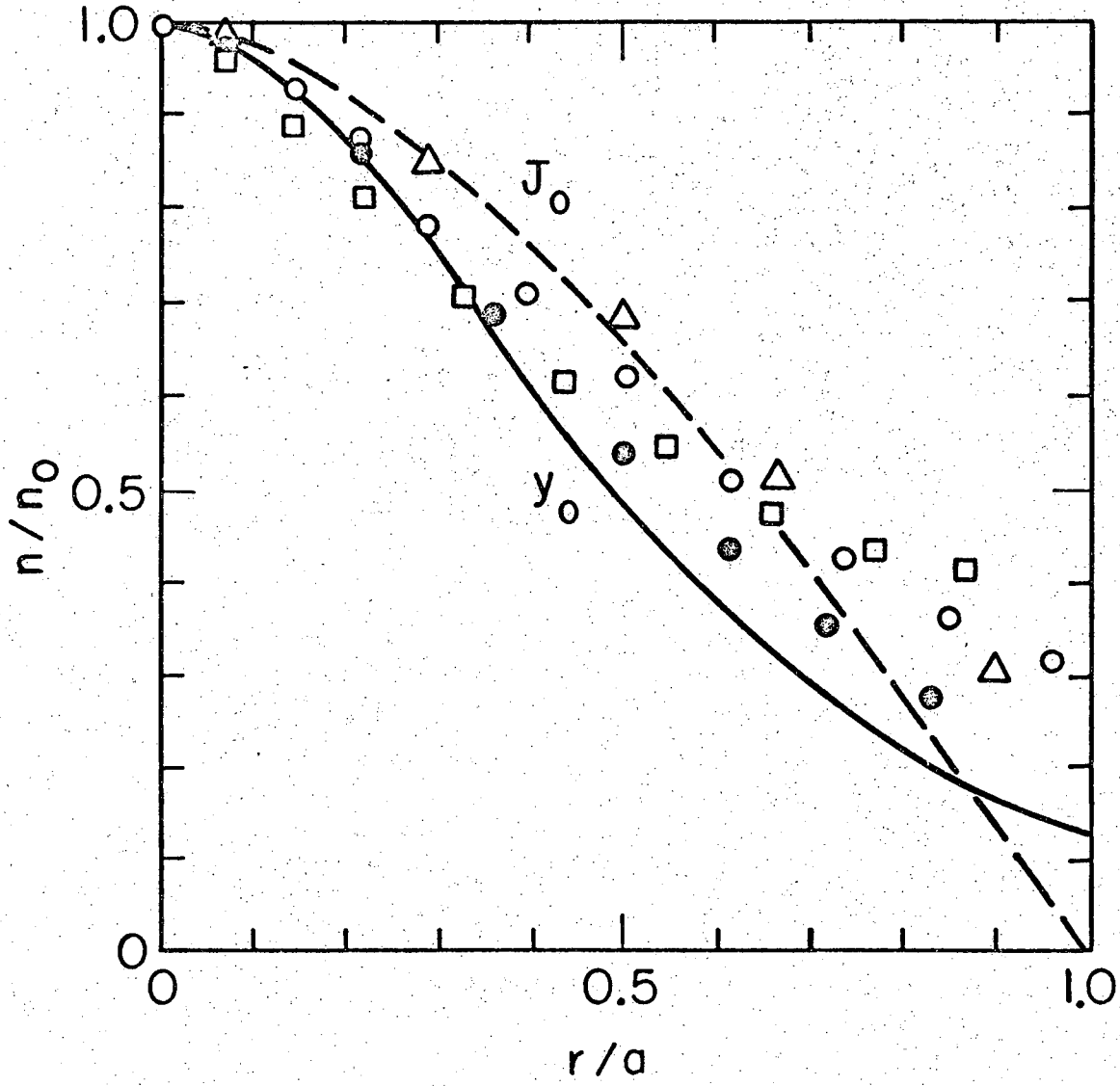
XBL697-3169

Fig. 1



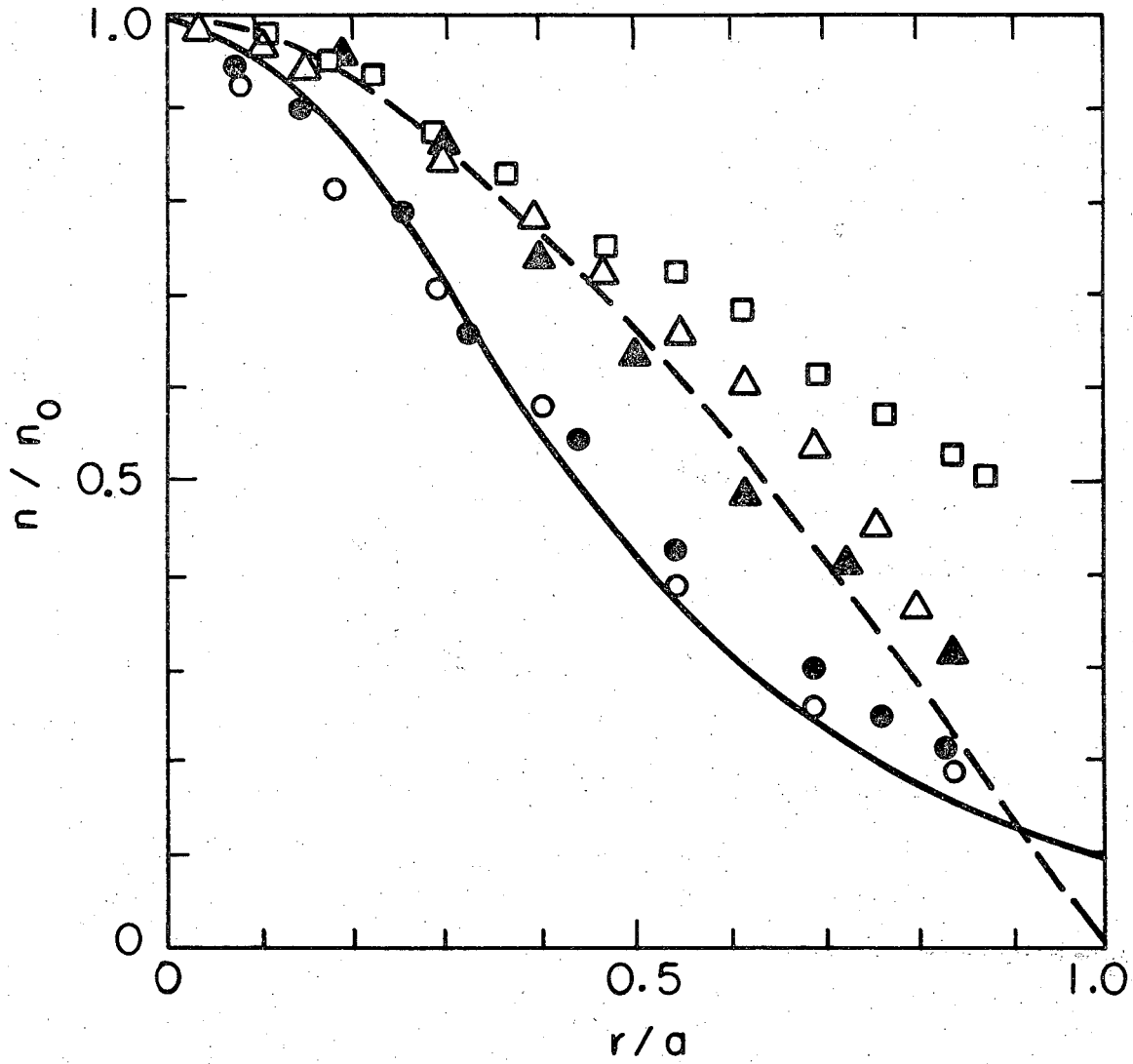
XBL697-3170

Fig. 2



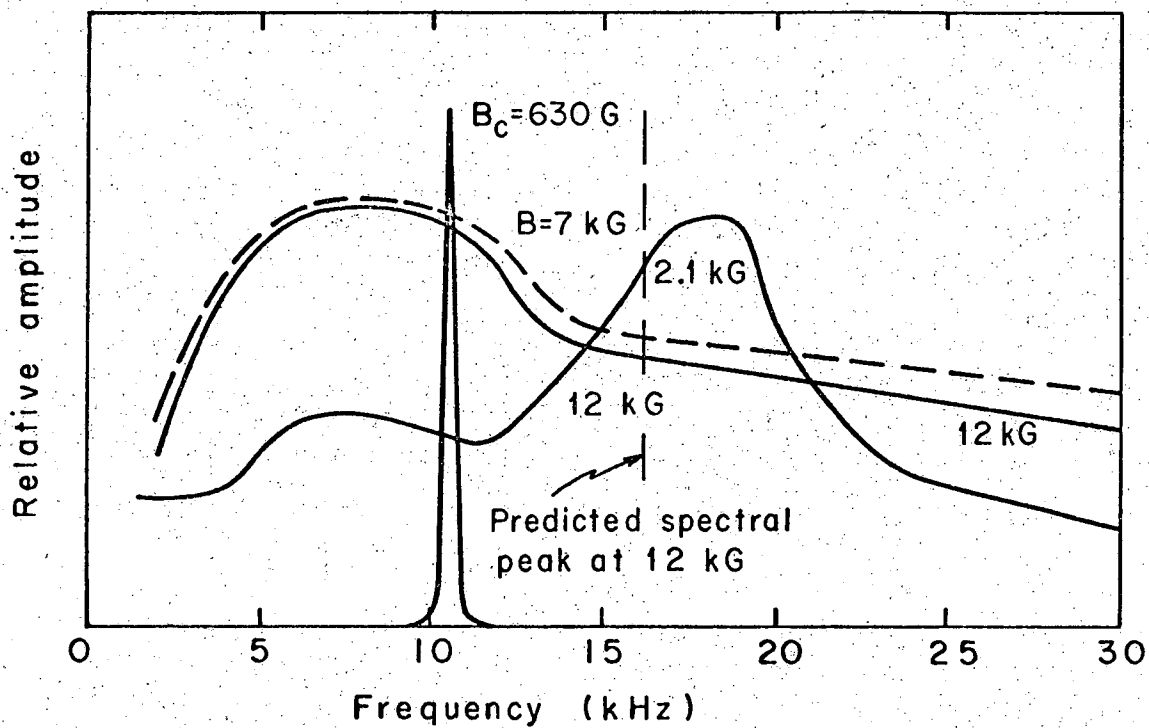
XBL697- 3171

Fig. 3



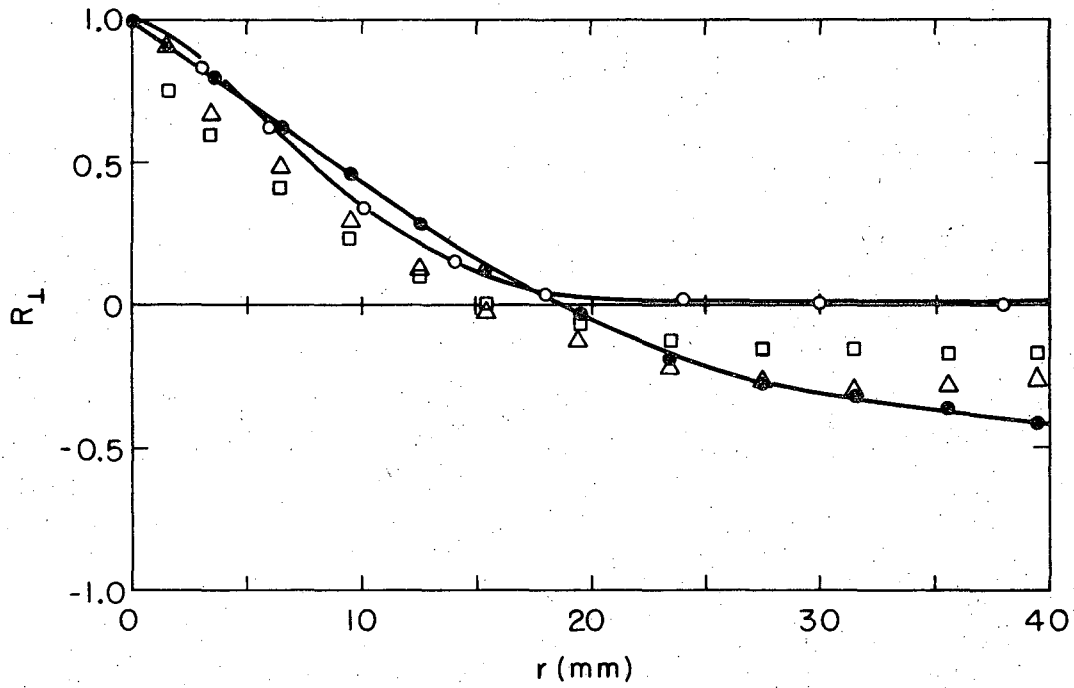
XBL697-3172

Fig. 4



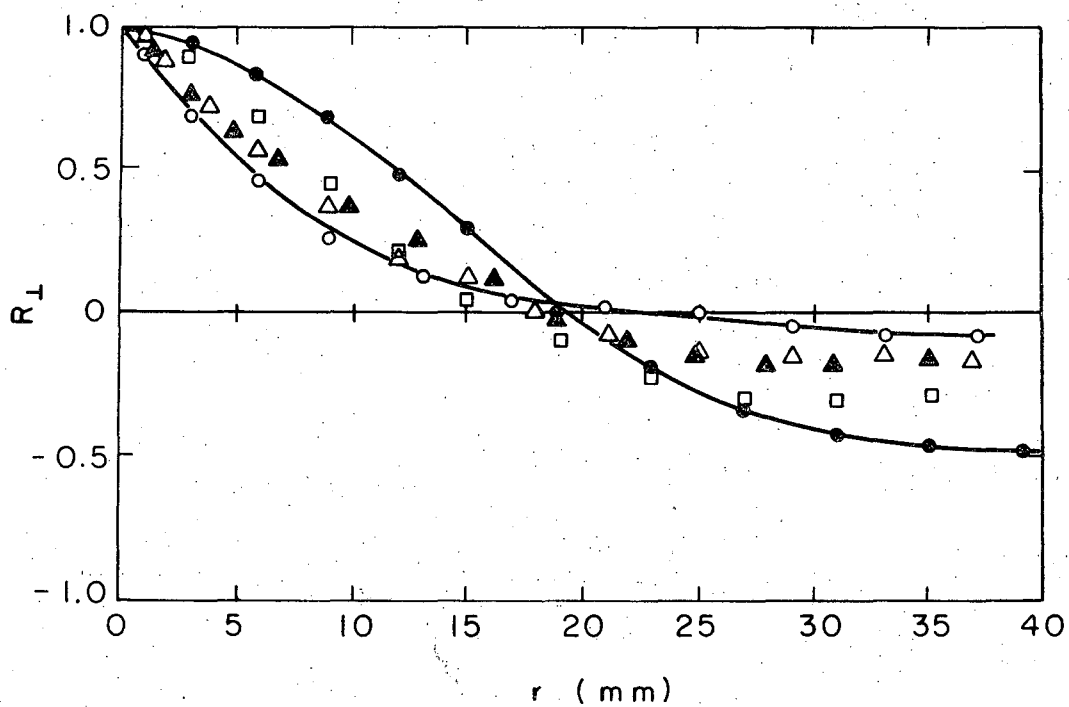
XBL697-3162

Fig. 5



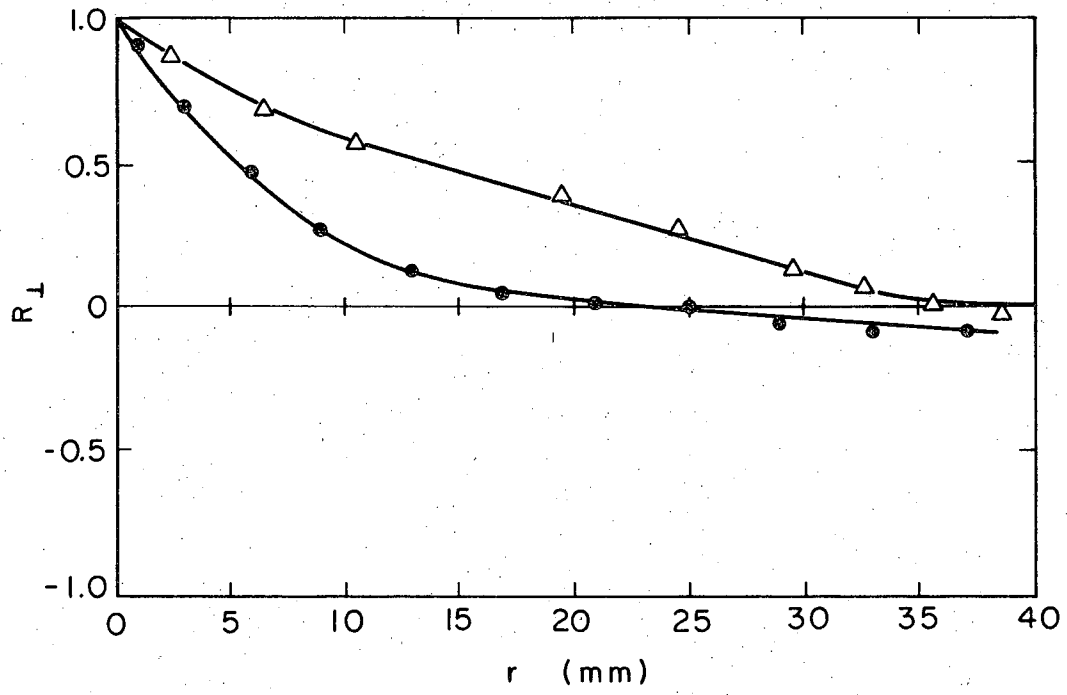
XBL697-3163

Fig. 6



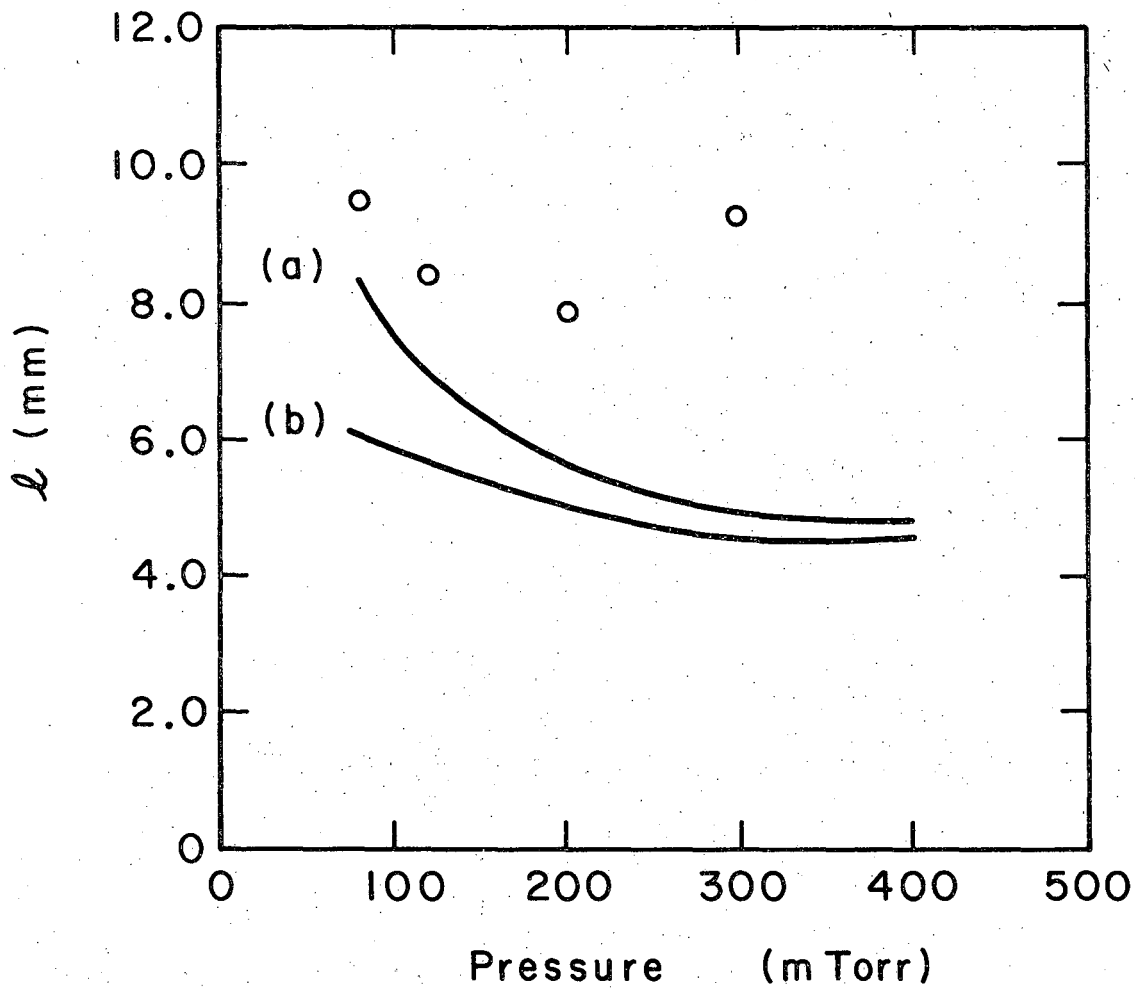
XBL697-3164

Fig. 7



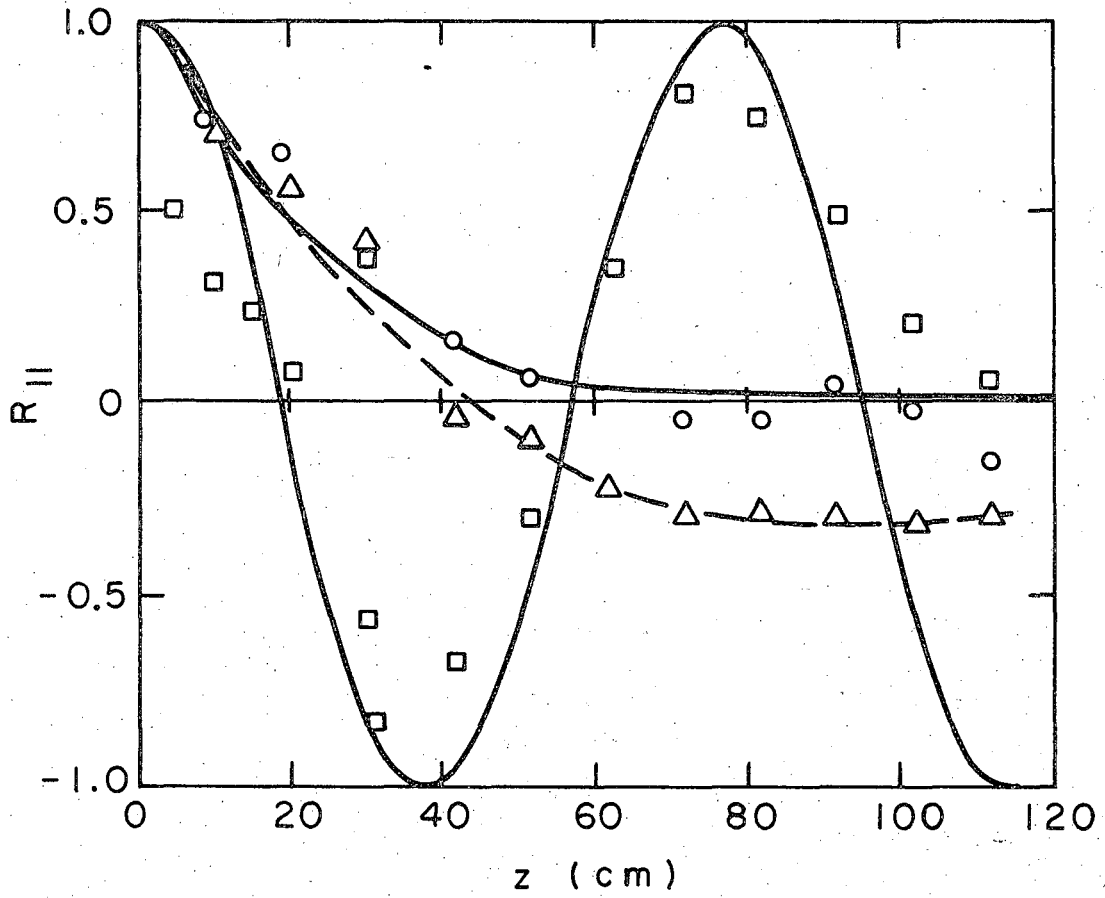
XBL697-3166

Fig. 8



XBL697-3167

Fig. 9



XBL697-3168

Fig. 10

LEGAL NOTICE

This report was prepared as an account of Government sponsored work. Neither the United States, nor the Commission, nor any person acting on behalf of the Commission:

- A. Makes any warranty or representation, expressed or implied, with respect to the accuracy, completeness, or usefulness of the information contained in this report, or that the use of any information, apparatus, method, or process disclosed in this report may not infringe privately owned rights; or*
- B. Assumes any liabilities with respect to the use of, or for damages resulting from the use of any information, apparatus, method, or process disclosed in this report.*

As used in the above, "person acting on behalf of the Commission" includes any employee or contractor of the Commission, or employee of such contractor, to the extent that such employee or contractor of the Commission, or employee of such contractor prepares, disseminates, or provides access to, any information pursuant to his employment or contract with the Commission, or his employment with such contractor.

TECHNICAL INFORMATION DIVISION
LAWRENCE RADIATION LABORATORY
UNIVERSITY OF CALIFORNIA
BERKELEY, CALIFORNIA 94720